Accepted Manuscript

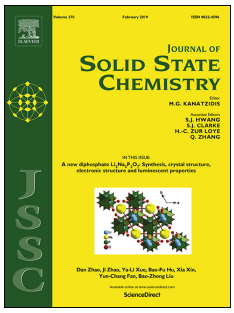

Mechanochemical reactions of alkali borohydride with CO_2 under ambient temperature

Wei Zhu, Juan Zhao, Lu Wang, Yun-Lei Teng, Bao-Xia Dong

PII: S0022-4596(19)30371-8

DOI: https://doi.org/10.1016/j.jssc.2019.07.037

Reference: YJSSC 20876

To appear in: *Journal of Solid State Chemistry*

Received Date: 27 March 2019

Revised Date: 17 July 2019

Accepted Date: 21 July 2019

Please cite this article as: W. Zhu, J. Zhao, L. Wang, Y.-L. Teng, B.-X. Dong, Mechanochemical reactions of alkali borohydride with CO_2 under ambient temperature, *Journal of Solid State Chemistry* (2019), doi: https://doi.org/10.1016/j.jssc.2019.07.037.

Mechanochemical reactions of alkali borohydride with CO_2 under ambient temperature

wei zhu; juan zhao; lu wang; Yun-Lei Teng *; baoxia dong *;

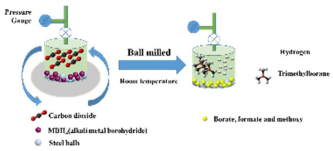

Mechanochemical reactions of alkali borohydride with CO_2 under ambient temperature

Wei Zhu, Juan Zhao, Lu Wang, Yun-Lei Teng,* Bao-Xia Dong*

School of Chemistry and Chemical Engineering, Yangzhou University, Yangzhou, 225002, P. R. China.

Abstract: Many efforts have been made to study the reactions of the borohydride with CO_2 in solution. However, it is scarce to achieve the hydrogenation of CO_2 using borohydrides as hydrogen source by the solid-gas direct reaction in the condition of ball milling under ambient temperature. Herein, we investigated the solid-gas noncatalytic reaction of ABH_4 (A = Li or Na) with CO_2 under mechanochemical conditions for the first time. It is found that hydrogen and trimethylborane are formed in the gas phase, as well as borate, formate, and methoxy species are formed in the solid phase.

Keywords: Carbon dioxide; Borohydride; Ball milling; Ambient temperature

*Corresponding author. E-mail: ylteng@yzu.edu.cn; bxdong@yzu.edu.cn.

1. Introduction

As the increasing use of carbon-based fuels by humans, the amount of carbon dioxide (CO_2) emitted to the atmosphere has also risen sharply. The vast amount of CO_2 causes significant and negative effects on the global environment [1]. In 2016, the volumetric concentration of CO_2 in the earth's atmosphere exceeded 400 ppm for the first time, which was much higher than the 280 ppm before industrialization [2]. Therefore, it is important to take effective measures to reduce and treat CO_2 emissions. As an economical, safe, and sustainable carbon resource compound, CO_2 has great potential for development into liquid fuels and chemicals which conforms to the green chemistry principles [3-5].

Borohydrides are conventional hydride-donating agents in use today. The chemical properties of borohydride are affected by bonding between metallic atoms and borohydride ligands and the electron structure. The H in $[BH_4]^-$ is mainly bonded to B by a covalent bond, resulting in that the thermodynamic properties are very stable [6,7]. Therefore, borohydrides often exhibit different property with that of salt-like hydrides such as LiH, NaH, and MgH_2. Borohydrides have been widely used in organic synthesis to reduce various functional groups because they are stable reduction reagents in air and solution [8,9]. In addition, due to their high weight energy densities. Borohydrides are also widely used ad hydrogen source. A significant effort has been made to produce hydrogen by hydrolysis or by combining with other

hydrides [10-14].

Recently, many efforts have been made to study the reactions of the borohydride with CO_2 in solution. Kyle et al. reported that sodium borohydride ($NaBH_4$) could react with CO_2 and bicarbonate (HCO_3^-) in aqueous solution to form formate ($HCOO^-$) [15]. Zhao et al. have developed a process for converting CO_2 to $HCOO^-$ using sodium borohydride at 318 k in a solution of the PH of 9.0 [16,17]. Waheed et al. achieved the reduction of CO_2 to ethanol by a two-step process using methyl magnesium bromide CH_3MgBr (Grignard reagent) and sodium borohydride in tetrahydrofuran [18]. Knopf et al. reported that sodium borohydride in butyronitrile solution could be used to reduce CO_2 to formate without the use of expensive borane or complex catalysts [19]. Hao et al. used $NaBH_4$ as a reducing agent in dimethyl sulfoxide to achieve reductive acylation of amine and CO_2 at 100 °C without a catalyst, resulting in a series of formylation products [20]. Fletcher et al. provided an efficient method for producing formic acid in high yield (24%) by reducing CO_2 with potassium borohydride(KBH_4) in aqueous solution under ambient conditions [21]. Sabet-Sarvestani et al. explored the reduction of CO_2 to methanol utilizing borohydride compounds as a reducing agent [22].

During investigating reactions between borohydride and CO_2, the reduction of CO_2 to carbon by solid-solid and solid-gas interaction are also explored. Lou et al. synthesized Y-junction carbon nanotubes by reducing CO_2 with $NaBH_4$ at 700 °C [23]. Vitillo et al. found that the main products in the reaction of γ-$Mg(BH_4)_2$ with CO_2 are formate and alkoxide compounds [24]. Zhang et al. found that sodium borohydride

reacted with CO_2 at 500 °C to produce boron-doped porous carbon [25]. Zhang et al. also demonstrated that under moderate conditions, CO_2 could be reduced to graphene oxide using ammonia borane by two consecutive steps [26]. Picasso et al. studied the solid-gas noncatalytic reaction between KBH_4 and CO_2 under thermal induction conditions and found potassium formyl hydroborate, K $[H_xB(OCHO)_{4-x}]$ (x = 1-3), is the main product [27].

However, it is scarce to achieve the hydrogenation of CO_2 using borohydrides as hydrogen source by the direct solid-gas reaction in the condition of ball milling under ambient temperature. We believe that the solid-gas reaction proceeded by mechanochemistry is convenient, safe, and scalable. Besides, little attention in previous experiments was paid to the gaseous products released from the reaction between borohydride with CO_2. In this work, we studied the reactions between ABH_4 (A = Li or Na) and CO_2 in the absence of a catalyst under mechanochemical conditions. It is found that hydrogen and trimethylborane are formed in the gas phase, as well as borate, formate, and methoxy species are formed in the solid phase.

2. Experimental methods

2.1 Materials

Lithium borohydride ($LiBH_4$) with a purity of 97% was obtained from Aladdin. Sodium borohydride ($NaBH_4$, 98%) was supplied by Shanghai Ruihua Chemical Co. Ltd. Carbon dioxide (CO_2 with a purity of 99.999%) was acquired from Shanghai Chemical Industry Park Pujiang Special Gas Co. Ltd.

2.2. The mechanochemical solid-gas reaction of ABH_4 (A = Li or Na) with CO_2

The mechanochemical solid-gas reaction of ABH_4 (A = Li or Na) with CO_2 was performed in an 80 mL stainless steel grinding bowl using a planetary ball milling apparatus (QM-3SP4) at 450 rpm. ABH_4 and CO_2 at the initial ratio of 1:1 mol/mol with 30 stainless steel balls (6 mm diameter, about 27 g) were used to ball mill. The initial pressure of CO_2 is controlled at 0.25 MPa by a pressure sensor. Moreover, the mass of $LiBH_4$ and $NaBH_4$ is 0.1787 g and 0.3104 g, respectively. ABH_4 and CO_2 were ball milled for 23 cycles, with a cycle duration of 1 hour and a pause of 30 min.

2.3. Characterization of gaseous product

The gaseous products were analyzed by gas chromatography (GC). H_2 concentration was detected using an SP-6890 GC (Rainbow Instrument Co., China) equipped with a TDX-01 column and a thermal conductivity detector (TCD). The gas Infrared spectroscopy was performed to characterize the gas product. The gas was introduced into the glass tube with potassium bromide at both ends. The gas Fourier transform IR spectroscopy (FTIR) were recorded on Bruker Vertex 70 v spectrometer between 500–4000 cm^{-1} and with a spectral resolution of 4 cm^{-1} in the transmission mode.

2.4. Characterization of solid product

The morphologies of the solid products were examined via scanning electron microscopy (SEM, S-4800II, Japan). Samples S-4800II analyses were placed on the sample holders supported by carbon paint followed by 1-min sputter coating of gold.

EDX analysis was accomplished using a link attachment on an S-4800II transmission electron microscope. Powder X-ray diffraction (XRD) measurement was carried out using an X-ray diffractometer (AXS D8 ADVANCE, Bruker, Germany) for a 2θ range of 10–80º, a step size of 0.1º and using graphite monochromatic Cu Kα radiation with a nickel filter. The tube current was 300 mA with a tube voltage of 40 kV. FTIR (Fourier-transform infrared) spectra were recorded on a Bruker TENSOR27 FTIR at a resolution of 4 cm^{-1} from 500 to 4000 cm^{-1}. ^{11}B and ^{13}C solid-state MAS NMR (magic angle spinning-nuclear magnetic resonance) spectra were recorded by Bruker AVANCE III400MHzWB, operating in a 9.4 T magnet. Samples were spun at 10 kHz for ^{11}B and 9 kHz for ^{13}C with the sample temperature maintained at 298.15 K. The ^{13}C solid-state MAS NMR spectra were referenced to the methylene carbon of adamantane at 38.48 ppm. ^{11}B NMR spectra were referenced against an external BF_3•OEt_2 standard (d = 0 ppm). All data were processed with 100 Hz line broadening.

3. Results and discussion

3.1. Gaseous product

ABH_4 (A = Li or Na) and CO_2 (0.25 MPa) were ball milled at 450 rpm during different reactions times. To elucidate the reaction process, we analyzed the gaseous products using GC. Distinct chromatographic peaks of hydrogen (at the retention time of around 0.28 min) are observed, as shown in Fig. 1. The peak intensity of H_2 in the ABH_4 (A = Li or Na)-CO_2 system increases with ball milling time increasing. The detector used in gas chromatography is a thermal conductivity detector (TCD), which

has low sensitivity and cannot detect a small amount of trimethylborane and other boron products.

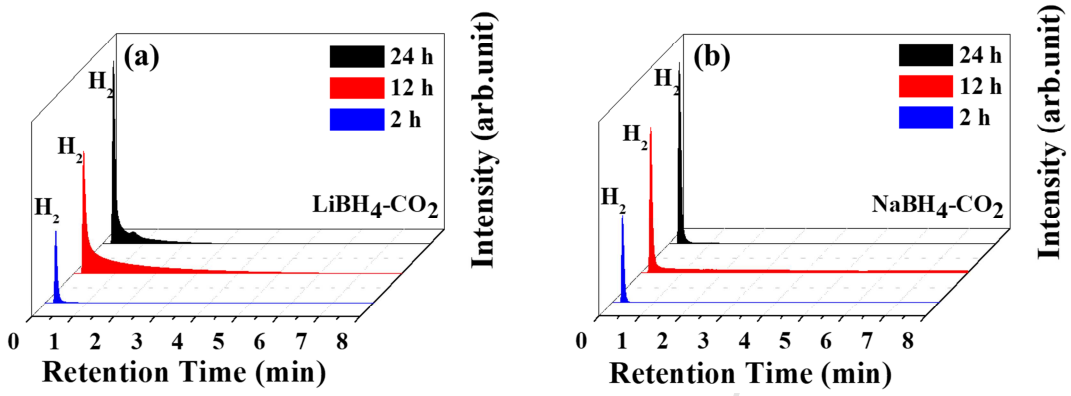

Fig. 1. GC profiles (tested with a TDX-01 column) of the gaseous products from the reaction between $LiBH_4$ ($NaBH_4$) and CO_2 for 2, 12, and 24 h.

In order to further determine the gas composition, FTIR spectra of the gaseous products from the reactions of ABH_4 (A = Li or Na) with CO_2 by ball milling were obtained (Fig. 2). The FTIR absorptions due to trimethylborane ($B(CH_3)_3$) were clearly observed at 2971, 2885, 1494, 1363, and 1041 cm^{-1}, which indicates that $B(CH_3)_3$ is formed in the reactions of ABH_4 (A = Li or Na) with CO_2 [28]. Moreover, FTIR spectra of the gaseous products from the $LiBH_4$-CO_2 system shows the difference from those of the $NaBH_4$-CO_2 system. Some adsorptions clearly reveal the formation of boron species containing B−H (peaks in the 2626 cm^{-1} region is due to ν(B−H), at 1619 cm^{-1} is due to γ(H−B−H) and around 1187 cm^{-1} is as result of ν(B−B)) [29].

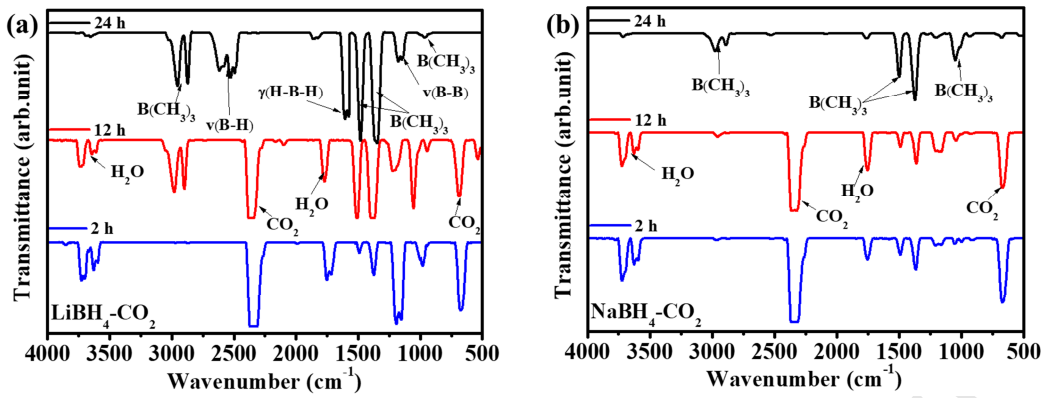

Fig. 2. IRGA (infrared gas analysis) of the gaseous products from the reaction between $LiBH_4$ ($NaBH_4$) and CO_2 for 2, 12, and 24 h.

This result indicates that the main gaseous products from the $LiBH_4$-CO_2 and $NaBH_4$-CO_2 systems are hydrogen and trimethylborane. As shown in Scheme S1, the trimethylborane species is possible to be formed due to the interaction of the B atom with the C atom forming an intermediate with B-C bond, which is further hydrogenated to form the trimethylborane species. Previous studies reported that methane could be largely prepared by the reactions of metal hydrides with CO_2 [30,31]. However, there is no methane after the reactions of borohydrides with CO_2. These results imply that the mechanism of the reaction of borohydrides with CO_2 is different from that of the reaction between metal hydrides and CO_2.

3.2. Solid product

Compared with the gaseous product after the reactions for 2 and12 h, there is no CO_2 in the gaseous product after the reaction for 24 h (Fig. 2). Therefore, the product after the 24-h reaction is selected for analysis and characterization. To further elucidate the reaction process, we characterized the solid products by FTIR, XRD,

and NMR.

The FTIR spectra of the solid products from the reaction between $LiBH_4$ ($NaBH_4$) and CO_2 are displayed in Fig. 3. For the $LiBH_4$-CO_2 system, the IR spectra are relatively simple. The peak at 2289 cm^{-1} is characteristic of ν(BH_4). The FTIR absorptions are clearly observed at 1627, 1375, 1006, and 698 cm^{-1}, which implies the formation of ν(C=O), ν(B−O), ν(B−O), and γ(B−O) [32]. According to the existing literature [32], the infrared telescopic vibration of B-O mainly has the following four types: the infrared peak at 1450-1300 cm^{-1} is Asymmetric stretching of $B_{(3)}$-O (three coordinate boron); the infrared peak at 1150-1000 cm^{-1} is Asymmetric stretching of $B_{(4)}$-O (four coordinate boron); the infrared peak at 960-890 cm^{-1} is Symmetric stretching of $B_{(3)}$-O; the infrared peak at 890-740 cm^{-1} is Symmetric stretching of $B_{(4)}$-O. However, the IR spectra from the $NaBH_4$-CO_2 system is complex (Fig. 3b). The peaks at 2293 cm^{-1} and 1278 cm^{-1} are characteristic of ν(BH_4) and σ(BH_4). As shown in Fig. 3b, some of peaks clearly show the production of formate (–OOCH, peak at 1608 cm^{-1} is as a result of ν(C=O) mode) and methoxy species (–OCH_3, peaks in the 3000–2800 cm^{-1} region is as a result of ν(CH_3) and approximately 1130 cm^{-1} is as a result of ν(C–O)) [24]. Eventually, the absorption bands centering approximately 1350, 1000, 945, and 823 cm^{-1} were assigned to the ν(B−O) mode (in agreement with the results of the NMR spectrum as following) [32].

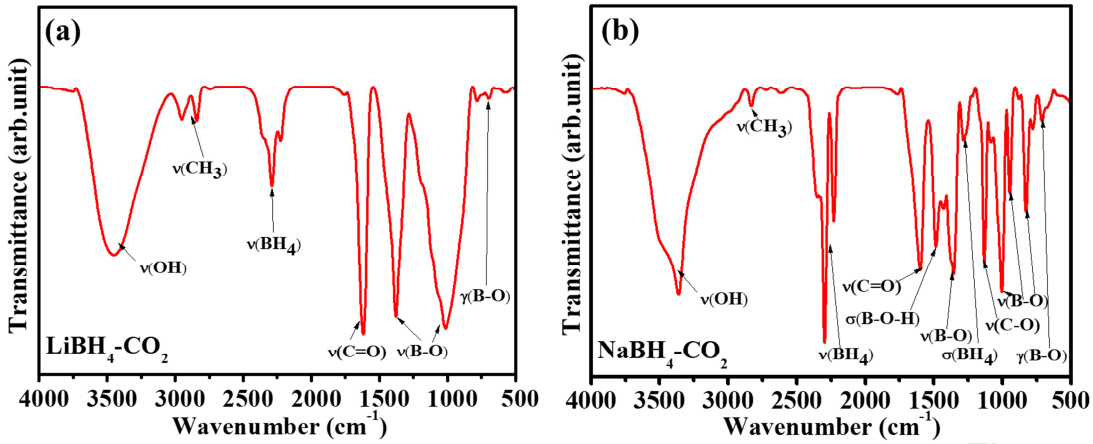

Fig. 3. FTIR spectra of the solid products from the reacton between $LiBH_4$ ($NaBH_4$) and CO_2 for 24 h.

The X-ray powder diffraction pattern of the solid-phase product is shown in Fig. 4. The $[BH_4]^-$ cannot be observed in XRD patterns (Fig. 4a), but the peak of ν(BH_4) is observed in Fig. 4a. However, Lang et al. studied the X-ray diffraction of unmilled and milled $LiBH_4$ [33]. They proved the crystal structure of $LiBH_4$ could not be destroyed. Therefore, we speculate the solid products of $LiBH_4$-CO_2 system is amorphous and attached to the surface of $LiBH_4$. For the $NaBH_4$-CO_2 system, Fig. 4b shows that $NaBH_4$ does not react completely (combined with Fig. 3b) after ball milling for 24 hours. There are no diffraction peaks due to new species, indicating that the solid products are amorphous.

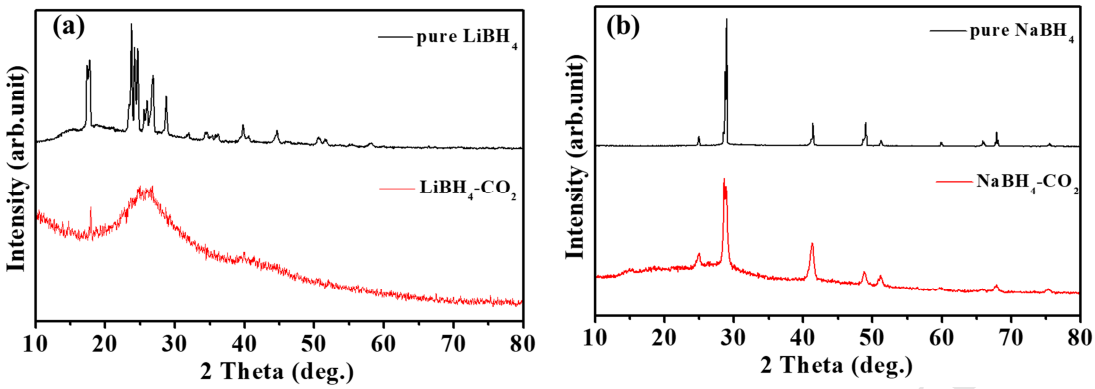

Fig. 4. XRD of the solid products from the reacton between $LiBH_4$ ($NaBH_4$) and CO_2 for 24 h.

The NMR spectra reveal the analogous information. The ^{13}C CP-MAS spectrum of the $LiBH_4$-CO_2 system (Fig. 5a) is characterized by peaks at 172.91, 85.61, and 50.83 ppm, which are characteristic of C=O, O−C, and OCH_3, further proving that there are formate and methoxy species in the solid products. This is in agreement with previous results [34]. Furthermore, the ^{13}C NMR spectrum of the $NaBH_4$-CO_2 system (Fig. 5b) is similar to the spectrum of the $LiBH_4$-CO_2 system (Fig. 5a).

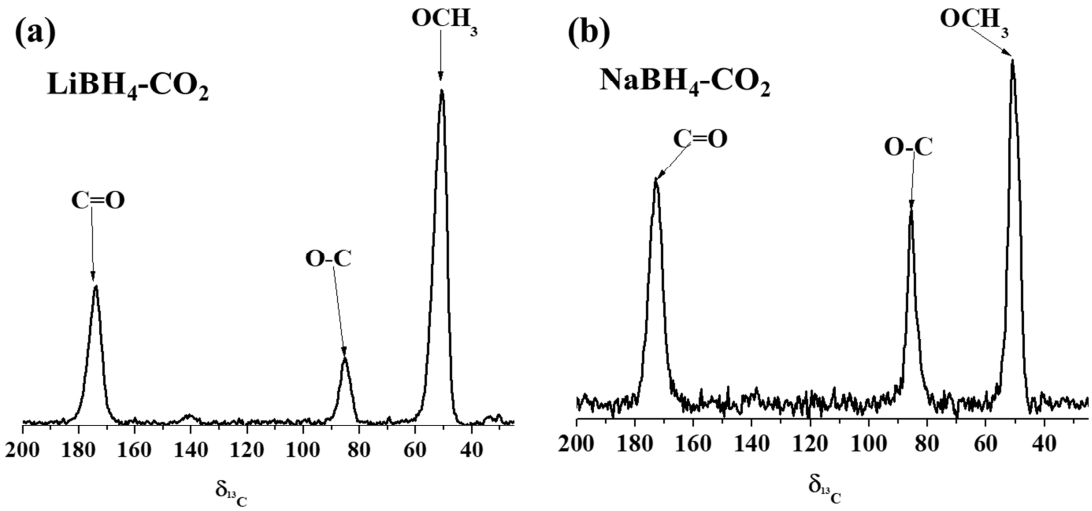

Fig. 5. The ^{13}C NMR spectra of the solid products from the reacton between $LiBH_4$ ($NaBH_4$) and CO_2 for 24 h.

Fig. 6 shows ^{11}B NMR spectra of the solid products formed in the reactions of ABH_4 (A = Li or Na) with CO_2. In the ^{11}B CP-MAS NMR spectrum of the $LiBH_4$-CO_2 system (Fig. 6a), sharp peaks at 0.78 ppm and -42.7 ppm are observed, corresponding to tetrahedral BO_4 groups (sp^3 B) and BH_4^- anion [21,26]. A weak peak at 13.37 ppm represents trigonal BO_3 groups (sp^2 B) in the NMR spectrum of the $LiBH_4$-CO_2 system [27]. Moreover, the ^{11}B NMR spectrum of the $NaBH_4$-CO_2 system (Fig. 6b) resembles the spectrum of the $LiBH_4$-CO_2 system (Fig. 6a). The unmarked peaks in Fig. 6 are rotating side-bands. The ^{11}B NMR spectra further prove that there are borate species in the solid products. Therefore, we speculate that the main solid-phase products are borate, formate, and methoxy species in the mechanochemical reaction of ABH_4(A = Li or Na) with CO_2, according to the characterizations of FTIR, XRD, ^{13}C NMR, and ^{11}B NMR. On the base of the analysis of the products and the reports in the literature [27], we tentatively proposed the formation mechanism of the borate, formate, and methoxy species by the reaction of borohydride with CO_2. As shown in Scheme S2, the formation of borate, formate, and methoxy species is most likely due to the transfer of hydride and the interaction of the boron atom and the oxygen atom. The peaks at 7.7 and 3.8 ppm in the ^1H CP-MAS spectrum of the $NaBH_4$-CO_2 system are probably due to characteristic of borate and methoxy species (Fig. S3), further demonstrating the presence of borate and methoxy species in solid products.

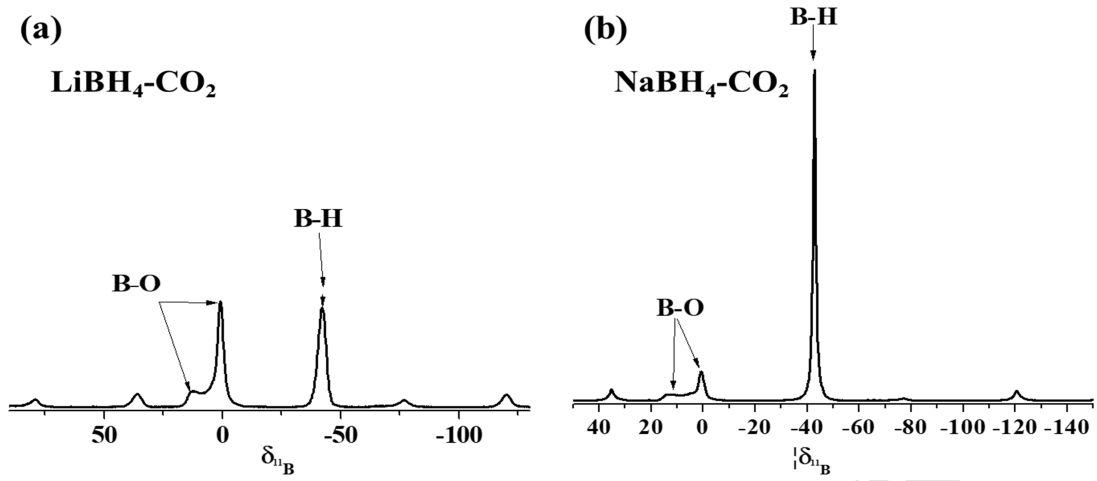

Fig. 6. The ^{11}B NMR spectra of the solid products from the reacton between $LiBH_4$ ($NaBH_4$) and CO_2 for 24 h.

4. Conclusion

In conclusion, the reactions of borohydrides with CO_2 under ambient-temperature ball milling condition were systematically studied firstly. The gas and solid products were characterized by GC, XRD, NMR, and FTIR. It is found that the reactions of borohydrides with CO_2 are complex, compared with the reactions of metal hydrides with CO_2. On the basis of experimental results, we infer that hydrogen and trimethylborane are formed in the gas phase, as well as borate, formate, and methoxy species are formed in the solid phase.

Acknowledgments

This work was supported by the National Natural Science Foundation of China (Nos. 21573192 and 21671169); the Priority Academic Program Development of Jiangsu Higher Education Institutions; and the High-Level Personnel Support Program of Yang-Zhou University.

References

[1] Hanak DP, Anthony EJ, Manovic V (2015) A review of developments in pilot-plant testing and modeling of calcium looping process for CO_2 capture from power generation systems. Energy Environ Sci 8:2199-22410.

[2] World Meteorological Organization (2017) WMO greenhouse gas bulletin: the state of greenhouse gases in the atmosphere based on global observations through 2016.

[3] Bhanage BM, Arai M (2014) Transformation and Utilization of Carbon Dioxide. Berlin: Springer.

[4] Yang J, Dong H (2016) CO_2-responsive aliphatic tertiary amine-modified alginate and its application as a switchable surfactant. Carbohydr Polym 153:1-6.

[5] Shi Q, Wu J, Mu S (2018) Direct experimental evidence and low reduction potentials for the electrochemical reduction of CO_2 on fluorine doped tin oxide semiconductor. J Electroanal Chem 820:1-8.

[6] Xu Z, Lin Z (1996) Transition metal tetrahydroborato complexes: an orbital interaction analysis of their structure and bonding. Coord Chem Rev 156:139-162.

[7] Ephritikhine M (1997) Synthesis, structure, and reactions of hydride, borohydride, and aluminohydride compounds of the f-elements. Chem Rev 97:2193-2242.

[8] Brown HC, Krishnamurthy S (1979) Forty years of hydride reductions. Tetrahedron 35:567-607.

[9] Nora de Souza MV, Alves Vasconcelos TR (2006) Recent methodologies mediated by sodium borohydride in the reduction of different classes of compounds. Appl

Organomet Chem 20:798-810.

[10] Demirci UB, Miele P (2009) Sodium borohydride versus ammonia borane, in hydrogen storage and direct fuel cell applications. Energy Environ Sci 2:627-637.

[11] Liu BH, Li ZP (2009) A review: hydrogen generation from borohydride hydrolysis reaction. J Power Sources 187:527-534.

[12] Ma J, Choudhury NA, Sahai Y (2010) A comprehensive review of direct borohydride fuel cells. Renewable Sustainable Energy Rev 14:183-199.

[13] Frommen C, Heere M, Riktor MD, Sørby MH, Hauback BC (2015) Hydrogen storage properties of rare earth (RE) borohydrides (RE = La, Er) in composite mixtures with $LiBH_4$ and LiH. J Alloys Compd 645:155-159.

[14] Kurko S, Aurora A, Gattia DM, Contini V, Montone A, Rašković-Lovre Ž, Novaković JG (2013) Hydrogen sorption properties of $MgH_2/NaBH_4$ composites. Int J Hydrogen Energy 38:12140-12145.

[15] Grice KA, Groenenboom MC, Manuel JDA, Sovereign MA, Keith JA (2015) Examining the selectivity of borohydride for carbon dioxide and bicarbonate reduction in protic conditions. Fuel 150:139-145.

[16] Zhao Y, Zhang Z, Wang H, Qian X (2016) Absorption of carbon dioxide by hydrogen donor under atmospheric pressure. Renewable Sustainable Energy Rev 64:84-90.

[17] Zhao Y, Zhang Z (2015) Thermodynamic properties of CO_2 conversion by sodium borohydride. Chem Eng Technol 38:110-116.

[18] Waheed H, Hussain A (2017) Utilization of Carbon dioxide (CO_2) for the

Production of Ethanol. J Chem Soc Pak 39:896.

[19] Knopf I, Cummins CC (2015) Revisiting CO_2 Reduction with $NaBH_4$ under aprotic conditions: Synthesis and characterization of sodium triformatoborohydride. Organometallics 34:1601-1603.

[20] Hao L, Zhang H, Luo X, Wu C, Zhao Y, Liu X, Liu Z (2017) Reductive formylation of amines with CO_2 using sodium borohydride: A catalyst-free route. J CO_2 Util 22:208-211.

[21] Fletcher C, Jiang Y, Amal R (2015) Production of formic acid from CO_2 reduction by means of potassium borohydride at ambient conditions. Chem Eng Sci 137:301-307.

[22] Sabet-Sarvestani H, Eshghi H, Izadyar M, Noroozi-Shad N, Bakavoli M, Ziaee F (2016) Borohydride salts as high efficiency reducing reagents for carbon dioxide transformation to methanol: Theoretical approach. Int J Hydrogen Energy 41:11131-11140.

[23] Lou Z, Chen C, Huang H, Zhao D (2006) Fabrication of Y-junction carbon nanotubes by reduction of carbon dioxide with sodium borohydride. Diamond Relat Mater 15:1540-1543.

[24] Vitillo JG, Groppo E, Bardají EG, Baricco M, Bordiga S (2014) Fast carbon dioxide recycling by reaction with γ-$Mg(BH_4)_2$. Phys Chem Chem Phys 16:22482-22486.

[25] Zhang J, Lee JW (2013) Production of boron-doped porous carbon by the reaction of carbon dioxide with sodium borohydride at atmospheric pressure. Carbon

53:216-221.

[26] Zhang J, Zhao Y, Guan X, Stark RE, Akins DL, Lee JW (2012) Formation of graphene oxide nanocomposites from carbon dioxide using ammonia borane. J Phys Chem C 116:2639-2644.

[27] Picasso CV, Safin DA, Dovgaliuk I, Devred F, Debecker D, Li HW, Filinchuk Y, 2016. Reduction of CO_2 with KBH_4 in solvent-free conditions. Int J Hydrogen Energy 41:14377-14386.

[28] Lehmann WJ, Wilson Jr CO, Shapiro I (1958) Characteristic Frequencies of Trimethylborane, J Chem Phys 28:777-780.

[29] Price WC (1948) The absorption spectrum of diborane, J. Chem. Phys. 16:894-902.

[30] Dong BX, Zhao J, Wang LZ, Teng YL, Liu WL, Wang L (2017) Mechanochemical synthesis of CO_x-free hydrogen and methane fuel mixtures at room temperature from light metal hydrides and carbon dioxide, Appl Energy 204:741-748.

[31] Zhao J, Dong BX, Teng YL, Wang L, Ping C, Li ZW (2018) Dehydrogenation reactions of mechanically activated alkali metal hydrides with CO_2 at room temperature, Int J Hydrogen Energy 43:5068-5076.

[32] Jun L, Shuping X, Shiyang G (1995) FT-IR and Raman spectroscopic study of hydrated borates, Spectrochim Acta Part A 51:519-532.

[33] Lang J, Gerhauser A, Filinchuk Y, Klassen T, Huot J (2012) Differential Scanning Calorimetry (DSC) and Synchrotron X-ray Diffraction Study of Unmilled and Milled $LiBH_4$: A Partial Release of Hydrogen at Moderate Temperatures. Crystals

2:1-21.

[34] Xiong R, Zhang J, Lee JW (2013) Carbon dioxide-facilitated low-temperature hydrogen desorption from polyaminoborane. J Phys Chem C 117:3799-3803.

Mechanochemical reactions of alkali borohydride with CO_2 under ambient temperature

wei zhu; juan zhao; lu wang; Yun-Lei Teng *; baoxia dong *

For the reaction of alkali borohydride with CO_2, hydrogen and trimethylborane are formed in the gas phase, as well as borate, formate, and methoxy species are formed in the solid phase.

Highlights

- The solid-gas reaction of alkali borohydride with CO_2 was investigated.
- The reaction is carried out at ambient temperature under mechanochemical condition.
- The hydrogen and trimethylborane are formed in the gas phase.
- The borate, formate, and methoxy species are formed in the solid phase.
- The work provides a new method for converting CO_2 using borohydrides.